2022

Optimal Load Shifting for Multiple ON/OFF Air Conditioning Units: How to Avoid Unnecessary Peak for Precooling?

Donghun Kim

James Braun

Optimal Load Shifting for Multiple ON/OFF Air Conditioning Units: How to Avoid Unnecessary Peak for Precooling?

Donghun Kim[1*], James E. Braun[2]

[1] Lawrence Berkeley National Laboratory, Building Technology & Urban Systems Deiision,
Berkeley, CA, USA
Contact Information (donghunkim@lbl.gov)
* Corresponding Author

[2] Purdue University, Mechanical Engineering,
West Lafayette, IN, USA
Contact Information (jbraun@purdue.edu)

ABSTRACT

Small and medium-sized commercial buildings (SMCB) are significant demand response resources, and it is important to develop grid-responsive control algorithms that exploit those resources and create financial benefits for building owners and HVAC service providers. Furthermore, unlike large-sized commercial buildings, there is an opportunity to have universally applicable control solutions for many SMCBs since those buildings have a consistent HVAC system configuration: SMCBs are commonly served by multiple-staged air conditioning units controlled by their own thermostats. Despite the demand response potential and scalability, however, very few control solutions are available for SMCBs. Typical model predictive control (MPC) and heuristic control approaches for cooling load shifting that lower thermostat setpoints before an electric price jump are suitable mainly for large-sized commercial buildings where a continuous capacity modulation is possible, e.g., via dampers in variable air volume terminal units. However, those approaches can cause undesired, high peaks for SMCBs due to the nature of ON/OFF unit staging and narrow thermostat deadbands. This could discourage the use of advanced grid-responsive controls for SMCBs due to the concern of high demand charges, and has to be resolved. This paper presents a MPC solution that overcomes this challenge. It has a hierarchical MPC structure where an upper level MPC is responsible for electrical load shifting in response to an electric price signal while a lower level MPC is responsible for coordinating compressor stages to eliminate unnecessary peaks and follows the setpoints determined by the upper level MPC. A comprehensive, long-term laboratory test has been carried out to demonstrate load shifting and evaluate cost savings of the algorithm.

1. INTRODUCTION

Since buildings account for over 70% of U.S. total electricity use, and contribute significantly to electric power demand peaks and carbon emission, integrating building controls with the grid can improve grid reliability, resiliency, and efficiency, and help in achieving states' and government's carbon neutrality goals. Buildings have inherent energy storage, i.e., the thermal mass associated with building structure, which can be used for shifting and shedding significant thermal loads. The use of thermal mass in cooling seasons can involve pre-cooling the building prior to an event (e.g., an ON peak price period) in order to lower cooling load and electric peak demand during the event. One of the most popular and widely studied control approaches for managing thermal mass is model predictive control (MPC), and a large number of previous studies have demonstrated that it can provide grid services while presenting economic benefits to building owners without compromising thermal comfort.

Small-sized ($< 464\ m^2$, $< 5,000\ ft^2$) and medium-sized ($< 4,640\ m^2$, $< 50,000\ ft^2$) commercial buildings (SMCB) account for about 95% of U.S. commercial buildings, 50% (3.6 billion m^2) of the total commercial indoor floor space and 60% of energy usage in the commercial building sector. Thus, SMCBs are undoubtedly tremendous, readily-available demand response resources. Furthermore, unlike large-sized commercial buildings, SMCBs have a fairly consistent HVAC and control configuration: commonly served by multiple staged air conditioning units, e.g., rooftop units (RTU), for space heating and cooling where each unit stage is controlled by its own thermostat. Examples are banks, retail stores, restaurants, schools and factories. This implies that there is a potential to have a universal and

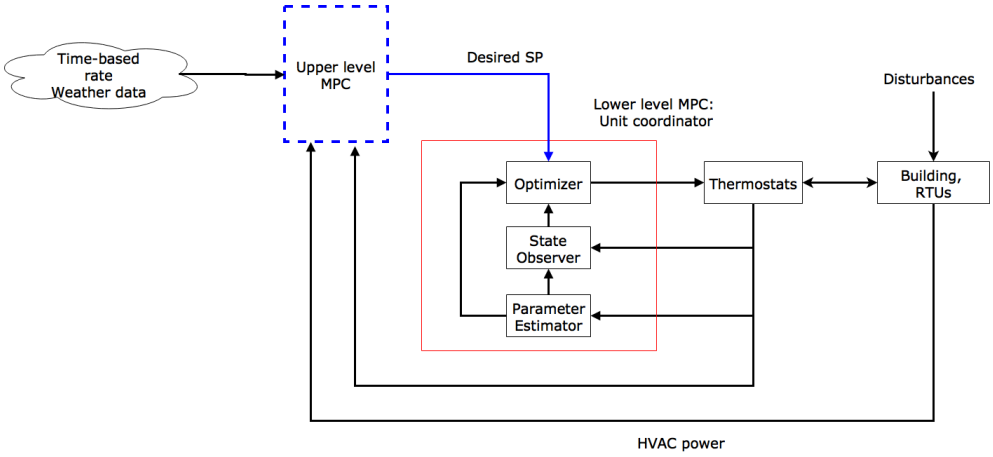

Figure 1: Conceptual diagram of a two-layer MPC for optimal load shifting and further peak demand reduction

scalable control solution which can be applied to many SMCBs and could rapidly transition them to Grid-interactive Efficient Buildings (GEB).

A limited number of MPC papers are found in the literature for SMCBs. Nutaro et al. (2014) developed a MPC algorithm and implemented it at a gymnasium having four identical 10-ton RTUs. This coordinator combines a simplified ARX type input-output model with heuristics and optimization to limit electric peak demand. The reduction of peak power consumption was about 15% with respect to a conventional thermostat control for the building. Kim et al. (2015) developed a MPC algorithm for minimizing energy consumption and electric peak demand for multiple RTUs especially for open-spaced buildings. The control approach was designed to minimize sensor and configuration requirements in order to enable a more cost effective control implementation for small/medium commercial buildings. It was implemented at a laboratory and muliple field sites, and reported overall up to 10% building HVAC energy savings and 20% peak demand reduction (Kim and Braun, 2018). Biyik et al. (2015) developed a RTU coordinator to minimize peak power. The goal was achieved by assigning different time varying penalties to different RTUs in order to prevent all units from operating simultaneously. It is reported that the peak power reduction with the optimal control strategy was about 20-40% for existing buildings. Putta et al. (2015) applied dynamic programming to solve an optimization problem for minimizing energy consumption and reducing compressor short cycling. In the case study, about 10% energy savings were estimated for a building served by 4 RTUs. Zhang et al. (2017) developed a RTU coordination control algorithm that shaves power usage within a limit during a demand response event for 90 minutes when triggered by a utility company, while minimizing comfort impacts.

However, those studies focus mainly on peak demand reduction and energy efficiency not load flexibility. SMCBs have a unique technical difficulty in load shifting. Typical MPC approaches in the literature, for variable air volume systems for example, which lower thermostat setpoints to shift load would not work for the type of buildings. This is because when the setpoints are lowered by, e.g., a couple of degree Celsius, full compressor stages for all units would be simultaneously activated creating a high electric peak due to the nature of ON/OFF stage of the units and narrow thermostat deadbands (usually $< 1^{o}C$). This is a very significant issue, since the undesired high peak and hence potentially high demand charge to building owners makes no economic sense for load shifting. To fully exploit SMCBs' demand response resources, this problem has to be solved.

This paper develops and demonstrates a MPC solution for SMCBs to overcome this problem. The solution incorporates a hierarchical MPC approach. Long-term experiments were carried out to demonstrate the load shifting and demand reduction capabilities. The MPC behaviors under two different time of use (TOU) scenarios were investigated, and one of the results for a typical TOU case is presented in this paper. Interesting trade-offs between energy efficiency and load flexibility were observed and are discussed.

2. METHODOLOGY: HIERARCHICAL MPC DESIGN

The proposed MPC for optimal load shifting for SMCBs has a hierarchical control structure as shown in Fig. 1 in which the upper level MPC (UMPC) marked with the blue dashed box optimizes desired setpoints while the lower level MPC (LMPC) marked with the red box acts as a slave controller. The UMPC is responsible for the optimal load shifting in response to utility price and weather signals by looking at long-term building thermal dynamics, while the LMPC optimally coordinates multiple RTUs or other unit packages to track the optimal setpoints determined by the UMPC while preventing unnecessary peaks discussed in the previous section.

2.1 Design of Lower MPC

In this section, mathematical descriptions of the LMPC are presented. It should be noted that the prediction horizon of the LMPC (N_p^L) is relatively short, e.g. 30 min to 1 hour. The control problem at a current time step k is:

$$\begin{aligned} \min \quad & \sum_{j=1}^{N_p^L}\sum_{i=1}^{p} P_i u_i(k+j-1) + \omega_d\delta + \omega_l\Gamma_l + \omega_u\Gamma_u \\ s.t. \quad & T_l^L - \Gamma_l \le E(y(k+j)|\mathcal{G}_k) \le T_u^L + \Gamma_u \\ & \sum_{i=1}^{p} P_i u_i(k+j-1) \le \delta \quad (\forall j \in \{1,\cdots,N_p^L\}), \end{aligned} \tag{1}$$

where j represents the time step for control changes measured from the current value of k. $u_i(k+j)$ and $y_i(k+j)$ represent unit stage and thermostat temperature for the i^{th} unit at the $k+j^{th}$ timestep. P_i is the rated power for the i^{th} unit. $E(y(k+j)|\mathcal{G}_k)$ is the optimal j-step prediction of thermostat temperatures given data $\mathcal{G}_k = \{y(k-1), y(k-2), \cdots, u(k+j-1), u(k+j-2), \cdots\}$. The prediction is calculated using the identified model, G_u (See Section **??**). $T_u^U (\in \mathbb{R}^n)$ are the desired setpoints that will be specified by the upper level MPC, and $T_u^L (\in \mathbb{R}^n)$ are temperature lower bounds. $\omega_l, \omega_u (\in \mathbb{R}^+)$ and $\omega_d (\in \mathbb{R}^+)$ are weights on variables of $\Gamma_l, \Gamma_u (\in \mathbb{R}^+)$ and $\delta (\in \mathbb{R}^+)$. Γ_l and Γ_u can be seen as comfort violations from the first constraint of (1) that are introduced to ensure a feasible solution. The variables to be optimized are the unit stages for all units over the prediction horizon and $\delta, \Gamma_l, \Gamma_u$, which form a mixed integer linear programming problem.

From the last constraint, it can be seen that δ is an upper bound on the electric demand for each time interval over the prediction horizon. Therefore, minimizing δ will naturally lower the electric peak demand over the prediction horizon. The coordination of unit stages to minimize the electric demand is the key component of the LMPC to eliminate high peaks for load shifting. For the capability of peak regulation and reliability of the LMPC, we refer to Kim and Braun (2018) which reports long-term field site MPC results.

2.2 Description of Upper MPC (UMPC)

In this section, mathematical descriptions of the UMPC are presented. To provide the optimal upper bounds (or desired cooling temperature setpoints) to the LMPC, i.e., T_u^L, it is natural to optimize setpoints by predicting a cost associated with the setpoints. However, it is challenging to obtain a dynamic model which maps setpoints to cooling load or power, because of the nonlinearity (hysteresis) of thermostats. Instead, an alternative approach is used: input trajectories are optimized first and desired setpoint trajectories are back calculated from the optimal inputs and G_u. With this in mind, the control problem of the UMPC at a current time step k is:

$$\begin{aligned} \min \quad & \sum_{j=1}^{N_p^U}\sum_{i=1}^{p} R(k+j-1)P_i(k+j-1)\bar{u}_i(k+j-1) \\ & + \omega_d\delta + \omega_l\Gamma_l + \omega_u\Gamma_u \end{aligned} \tag{2}$$

$$\begin{aligned} s.t. \quad & T_l^U - \Gamma_l \le E(\bar{y}(k+j)|\mathcal{G}_k) \le T_u^U + \Gamma_u \\ & \sum_{i=1}^{p} P_i(k+j-1)\bar{u}_i(k+j-1) \le \delta \\ & 0 \le \bar{u}_i(k+j-1) \le 1 \quad (\forall j \in \{1,\cdots,N_p^U\}), \end{aligned} \tag{3}$$

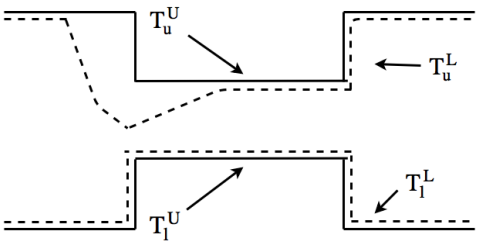

Figure 2: Example of upper and lower bounds for the UMPC and LMPC

where $\bar{u}$ and $\bar{y}$ are the moving averaged unit stages and thermostat temperatures, respectively, over a window (a 30-minute interval is used for this study). Because of averaging, $\bar{u}_i$ for each sampling time is a real number bounded by 0 and 1 (for a single stage unit): $\bar{u}$ can be viewed as unit runtime fractions (RTF) over the averaging window. A sequence of $\bar{u}(\cdot)$ is the optimization variable of (2). The desired setpoint trajectories are calculated with the optimal RTFs and an input-output model.

Differences compared with the LMPC formulation in (1) are explained as follows. N_p^U is the prediction horizon for the UMPC (> 6 hours), which is longer than N_p^L of the LMPC (around 1 hour). The control implementation time for the UMPC is also longer than that of the LMPC: That is, the UMPC and LMPC are implemented for every 30 min and 5 min, respectively. R which is the electricity rate is provided only to the UMPC for load shifting. The feedback and future prediction data set, i.e. $\mathcal{G}_k$, includes forecast of outdoor air temperature as follows. $\mathcal{G}_k = \{\bar{y}(k-1), \bar{y}(k-2), \cdots, \bar{u}(k+N_p^U-1), \bar{u}(k+N_p^U-2), \cdots, \bar{T}_o(k+N_p^U-1), \bar{T}_o(k+N_p^U-2), \cdots\}$ where $\bar{T}_o$ is the moving averaged signal with the same window size for $\bar{u}, \bar{y}$.

The upper and lower temperature bounds, i.e. T_l^U, T_u^U indicate an acceptable temperature range specified by users and are different from the bounds for the LMPC. The bounds for the LMPC could be narrower than that of the UMPC and are determined by the UMPC as follows.

$$T_{u,i}^L(k) = \begin{cases} \bar{y}_i^*(k), & \text{if } \bar{u}_i^*(k) > 0 \\ T_{u,i}^U(k), & \text{if } \bar{u}_i^*(k) = 0 \end{cases} \qquad (4)$$
$$T_{l,i}^L(k) = T_{l,i}^U(k), \ \forall i \in \{1, 2, \cdots, p\}$$

where $\bar{u}_i^*(k)$ indicates the optimal RTF over the averaging window for the i^{th} unit at the k^{th} timestep of the UMPC and $\bar{y}_i^*(k)$ is the corresponding desired temperature. The first equation of (4) means the desired temperature profiles are used for the upper bound for the LMPC. However, it is modified with the following heuristic strategy: if the UMPC does not use the i^{th} unit, i.e. $\bar{u}_i^*(k) = 0$, put the upper bound of the LMPC for the i^{th} unit as high as possible in order to turn off the unit.

Example profiles of the upper and lower bounds for the UMPC and LMPC are shown in Fig. 2. The bounds for the UMPC, solid lines in the figure, are based on a predefined temperature band while the bounds of the LMPC, dashed lines, follow a decision of the UMPC according to (4).

2.3 Modeling: System Identification

To predict zone air temperature profiles with a forecast for the outdoor air temperature and a candidate profiles of control inputs, we utilized a methodology termed the Lumped Disturbance modeling approach (LD) (Kim et al., 2016). We refer to Kim et al. (2018) for the mathematical description and background of the algorithm, and validation for the case study building of this paper.

3. LABORATORY TEST RESULTS

3.0.1 Site Description A cooling system for a conference room (about 15 m long, 7 m wide and 3.5 m high) in the Ray W. Herrick Laboratories at Purdue University, IN, U.S. (see Fig. 3) was retrofitted to test the overall MPC approach. Two packaged air conditioners (termed U1 and U2) were installed and the air duct system was reconfigured accordingly.

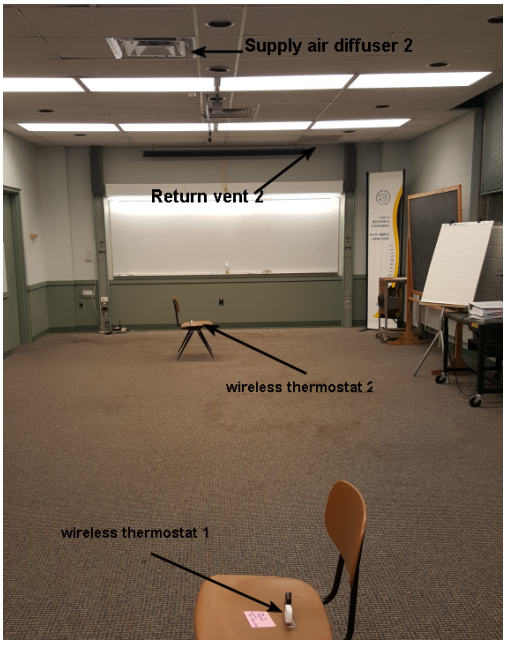

Figure 3: Case study building (supply air diffuser 1 and return vent 1 are not shown)

U1 is a 1-ton single stage unit with an energy efficiency ratio (EER) 9 and U2 is a 2-ton single stage unit with 10 EER. Thermostats, supply and return vents associated with the two units are shown in Fig. 3 and Fig. 4. Note that there is a strong coupling between the two sub-zones (or thermostats), and hence the operation of one unit can influence both thermostat temperatures. Unmeasured heat sources are lighting gains, loads from electric appliances (a small freezer and one laptop computer), infiltration/exfiltration, solar gains through windows, and occupancy gains. The lights were turned ON and OFF by occupant random behavior.

It should be noted that the conference room is not very representative of many SMCBs in the sense that 1) it has a carpet and mat (see Fig. 3) and 2) it has a high U-value for the wall and window (See the external view of Fig. 4): the external wall consists of pure bricks (without insulation) and single pane windows covering around 1/3 of the wall area. These system properties restrict the MPC savings potential which will be discussed in detail.

Conventional Control Set Up: A conventional thermostat control (Conv) turns on and off the unit stages based on thermostat deadband(s) and tracking error between the measured thermostat temperature and setpoint. The Conv fol-

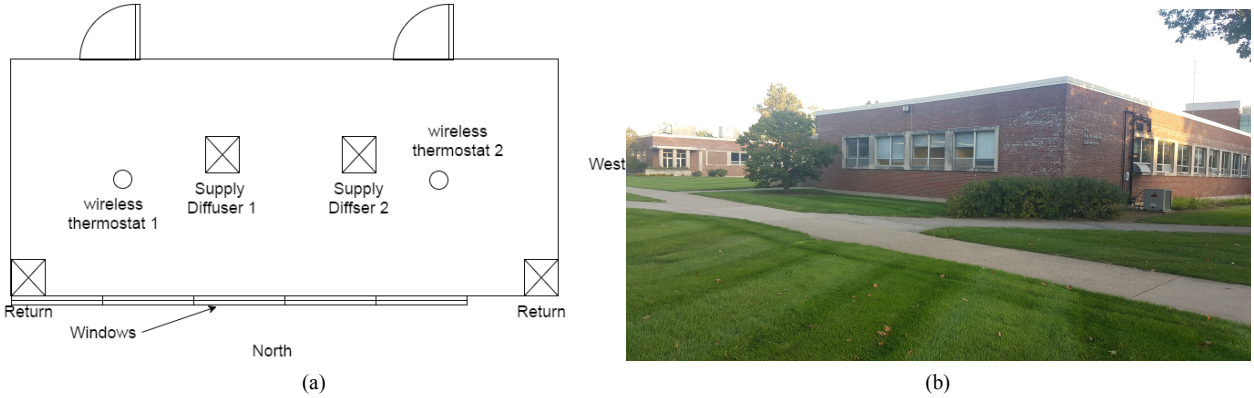

Figure 4: (a) Floor plan with locations of thermostats, supply diffusers and return vents and (b) external view of the demonstration site (Purdue Herrick Laboratory)

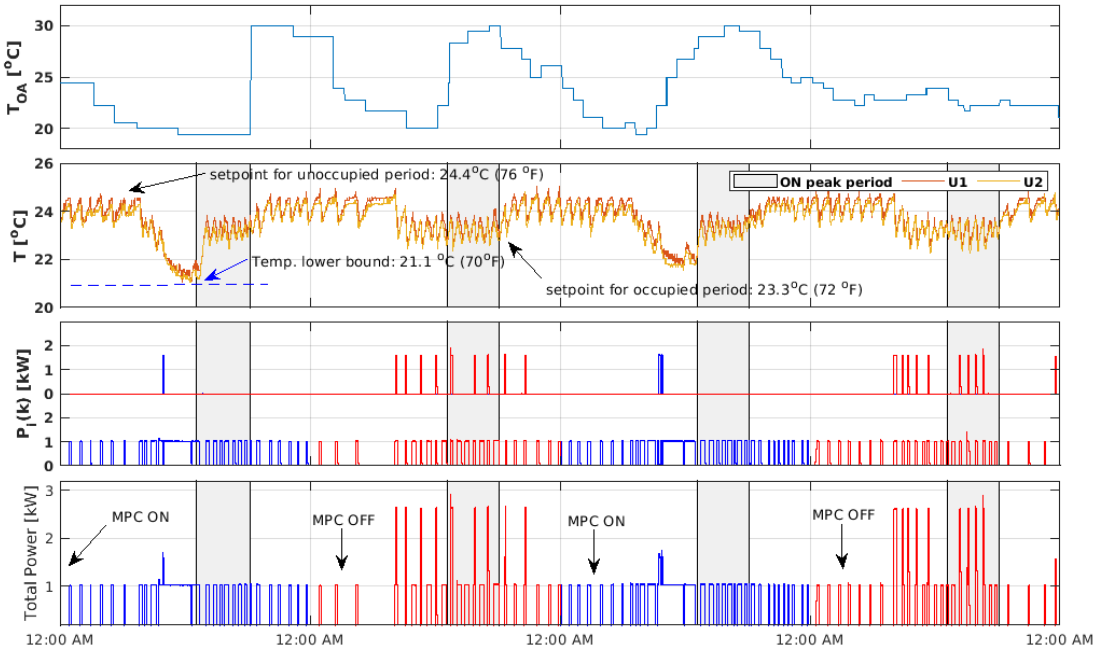

Figure 5: Sample profiles of outdoor air temperature, zone air temperature, setpoints, instantaneous unit powers, and total HVAC power under conventional control and MPC

lows a night setup schedule, 23.3^oC (74^oF) during the occupied period (9:00 AM to 6:00 PM) and 24.4^oC (76^oF) during the unoccupied period.

Hierarchical MPC Set Up: For the lower level MPC (LMPC), the sampling time for control implementation was 5 minutes and the prediction horizon was set to 40 minutes. For the upper level MPC (UMPC), the control implementation time interval and averaging window were set to 30 minutes with a 12-hour prediction horizon. The temperature upper limit (T_u^U) followed the same night setup schedule. That is, 23.3^oC (74^oF) during the occupied period and 24.4^oC (76^oF during the unoccupied period. The lower temperature limits for both LMPC and UMPC (T_l^U and T_l^L) were set to 21.1^oC (70^oF). The NOAA API was used to retrieve weather forecasts (using the Purdue airport weather station, which is around 1.5 miles away from the lab) for the UMPC's 12-hr ahead prediction and the forecast was updated every 30 min, which is the UMPC implementation time. Once a decision was made by the UMPC, it was applied to the LMPC according to Eqn. (4). Then, a stage decision was made by the LMPC, and was transmitted to the thermostats every 5 minutes, which is the control implementation time interval for the LMPC.

Utility Cost Setup: The utility cost is a key parameter that decides the behavior and energy cost savings of the MPC. A few different electricity rates were investigated, and in this paper the results for the following rate structure are presented.

- 0.20 $/kWh from 1:00 PM to 6:00 PM (the ON peak period), and 0.10 $/kWh at other times.

3.1 Experimental Test Results (ON-to-OFF peak price ratio of 2)

3.1.1 Experimental Results: Short-Term Comparison: Fig. 5 shows sample test results for 4 days for the conventional control and MPC on days in August under the ON-to-OFF peak price ratio of 2 and an on-peak period from 1:00 PM to 6:00 PM. As shown at the bottom of the figure, the two control algorithms were switched back and forth on a daily basis. Thermostat temperatures (blue line: U1, brown line: U2) are shown in the second subfigure. The unit powers are displayed in the third figure and the total HVAC power (a 15-min moving average) is shown in the last (red: conventional controller days, blue: the MPC days).

The temperatures in the second figure show that the MPC clearly responds to the on-off peak price signal (0.2 $/kWh

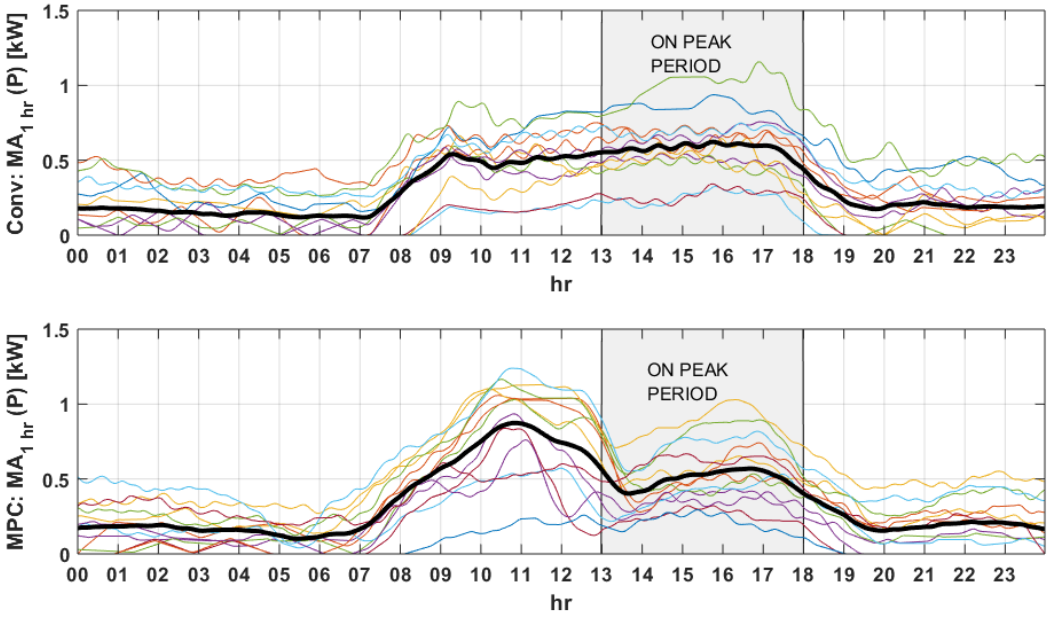

Figure 6: Distributions of daily profiles of total 1-hr moving average HVAC power for the conventional control and MPC. For each figure, different colors represent moving-averaged power measurements for different days, and the thick black line indicates the mean trajectory.

from 1:00 PM- 6:00 PM, 0.1 $/kWh elsewhere). The MPC precools the space down to the lower temperature limit (21.1^oC, 70^oF) when the electricity price is low, and turns off the units for a period after the price jumps. The precooling started at around 2 to 4 hours ahead of the price jump and the temperatures were smoothly lowered down. During the precooling periods, the peaks are under regulation as shown in the bottom of the figure.

3.1.2 Experimental Results: Long Term Comparison: Fig. 6 shows sets of daily HVAC power profiles (1-hr moving averaged) for the conventional and MPC. Fig. 7 shows comparisons of the two representative profiles between the two controllers. To ensure that the comparison of sampled powers is meaningful, daily temperature distributions are also provided in Fig. 8. Clearly, the MPC regulated thermostat temperatures within the specified temperature range (21.1 to 23.3^oC, 70 to 74^oF during the occupied period of 9:00 AM to 6:00 PM, and 21.1 to 24.4^oC, 70 to 76^oF during the unoccupied period). As shown in the last subfigure of Fig. 8, the MPC precooled the space to around 22.2^oC (72^oF) although the lower limit was set to 21.1^oC ($70\ ^oF$). This is due to the two conflicting driving potentials of the MPC, i.e., the utility cost rate structure and increment of loads from the outdoor air for precooling.

Fig. 7 demonstrates the electrical load shifting capability of the MPC. It shifts electrical loads for about 3 to 4 hours. The MPC gradually increases the charging until the price jump and it discharges after that. The discharging capacity is high at the beginning but drops exponentially. The discharging process is effective for around 4 hrs (1:00 PM – 5:00 PM). The increase of energy consumption associated with the precooling compared with that of the baseline is 9.77%.

The energy cost savings for this experiment was only 3.61%. As mentioned, the small energy cost savings are due to a significant thermal resistance between the zone air and building structure and poor insulation. Fig. 9 shows 15-min moving averaged total power profiles for the two controllers to compare peak demand charges. The MPC's anytime demand savings are 36% (compare the black dashed lines showing the maximum values for the two controllers). For the case of on-peak demand charge, savings are 60% (see the red dashed lines showing the maximum peaks over the on-peak period). The greater on-peak demand savings are the combined effect of reduced cooling loads due to precooling and the narrower on-peak period where the discharging is effective in addition to the LMPC's coordination effort.

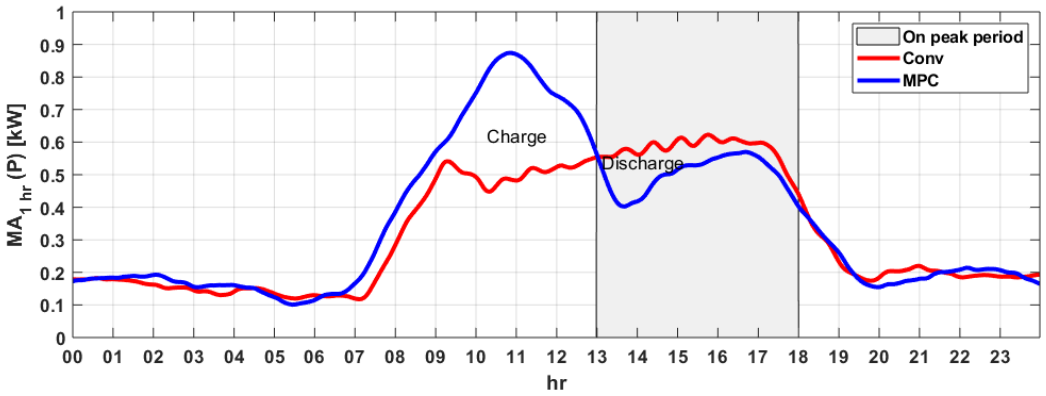

Figure 7: Comparison of representative daily profiles of total 1-hr moving average HVAC power between the conventional control and MPC

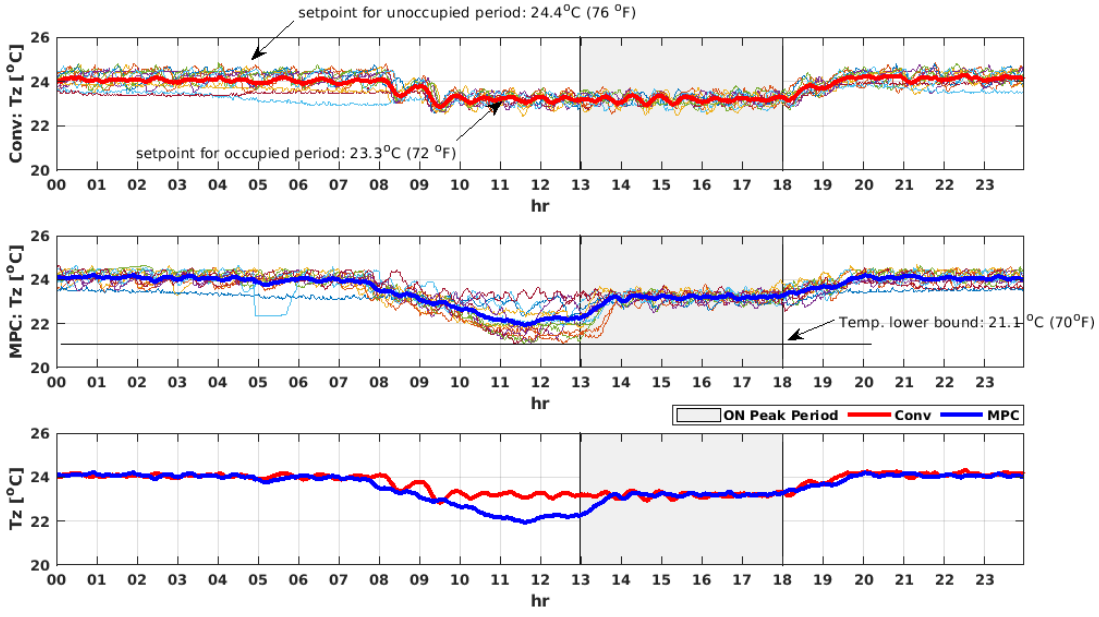

Figure 8: Distributions of daily temperature profiles between the conventional control and MPC. For each figure, different colors represent thermostat temperature measurements for different days, and the thick black line indicates the mean trajectory.

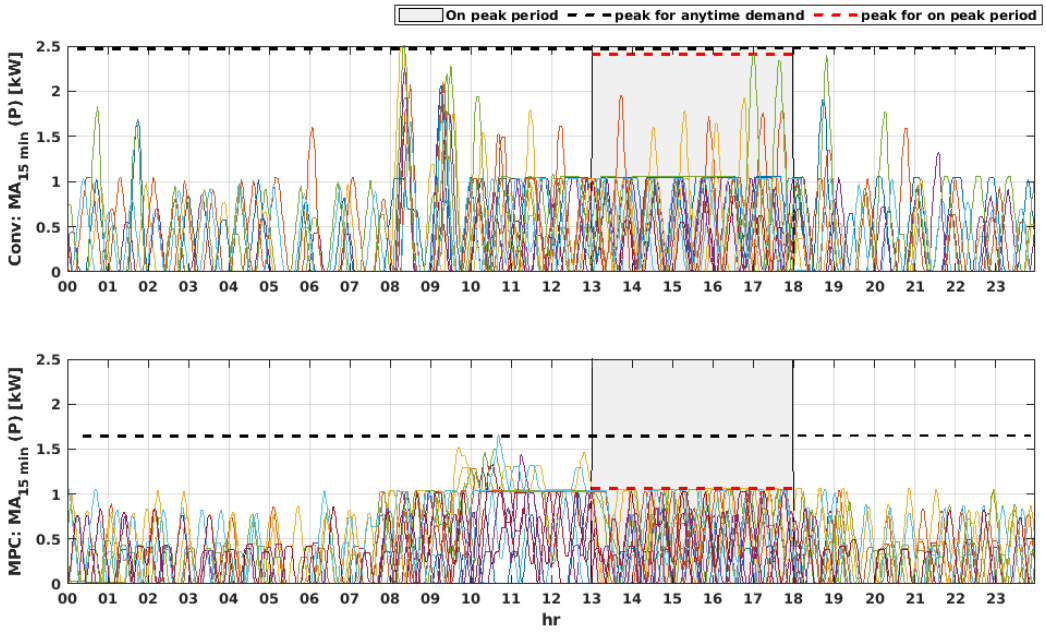

Figure 9: Distributions of daily profiles of total 15-min moving average HVAC power for the conventional control and MPC. For each figure, different colors represent moving-averaged power measurements for different days.

4. CONCLUSIONS

Despite a long history of studying MPCs applied to buildings and increasing needs for load flexibility in small and medium sized commercial buildings (SMCB), few advanced control algorithms have been developed for SMCBs. This paper discussed the unique MPC challenge of high peak demand occurring when shifting HVAC load for SMCBs served by multiple staged packaged air conditioners, and presented a hierarchical MPC to overcome this issue. The load shifting capability of the MPC while regulating the unnecessary peaks during precooling has been tested for a laboratory space over two months for two different time-of-use (TOU) scenarios. The MPC successfully shifted electrical loads in response to TOU rates, with remarkable HVAC demand cost savings, anytime demand cost savings over 30% and on-peak demand cost savings over 40%, but with only modest energy cost savings. The virtual battery, i.e. the building thermal mass, was effective for about 4-5 hours with a substantial load reduction during the ON peak period. The energy cost savings were less than 10%. One of the reasons for the low energy cost savings is the fact that the site has a carpet, mat and a poor envelope with single pane windows which results in inefficient charging and discharging of the building mass. It is expected that savings should be significantly greater for more typical commercial buildings.

REFERENCES

Biyik, E., Brooks, J. D., Sehgal, H., Shah, J., and Gency, S. (2015). Cloud-based model predictive building thermostatic controls of commercial buildings: Algorithm and implementation. In *American Control Conference (ACC), 2015*, pages 1683–1688. IEEE.

Kim, D., Braun, J., Cai, J., and Fugate, D. (2015). Development and experimental demonstration of a plug-and-play multiple rtu coordination control algorithm for small/medium commercial buildings. *Energy and Buildings*, 107:279–293.

Kim, D. and Braun, J. E. (2018). Development, implementation and performance of a model predictive controller for packaged air conditioners in small and medium-sized commercial building applications. *Energy and Buildings*, 178:49–60.

Kim, D., Cai, J., Ariyur, K. B., and Braun, J. E. (2016). System identification for building thermal systems under the presence of unmeasured disturbances in closed loop operation: Lumped disturbance modeling approach. *Building and Environment*, 107:169–180.

Kim, D., Cai, J., Braun, J. E., and Ariyur, K. B. (2018). System identification for building thermal systems under the presence of unmeasured disturbances in closed loop operation: Theoretical analysis and application. *Energy and Buildings*, 167:359 – 369.

Nutaro, J. J., Fugate, D. L., Kuruganti, T., and Starke, M. R. (2014). An inexpensive retrofit technology for reducing peak power demand in small and medium commercial buildings. Number 3494. Conference: 3rd International High Performance Buildings Conference at Purdue.

Putta, V., Kim, D., Cai, J., Hu, J., and Braun, J. E. (2015). A switched dynamic programming approach towards optimal control of multiple rooftop units. In *American Control Conference (ACC), 2015*, pages 281–287. IEEE.

Zhang, X., Pipattanasomporn, M., and Rahman, S. (2017). A self-learning algorithm for coordinated control of rooftop units in small-and medium-sized commercial buildings. *Applied Energy*, 205:1034–1049.

ACKNOWLEDGEMENT

The work was supported by the Center for High Performance Building (CHPB) at Purdue University, and completed with the support of the Assistant Secretary for Energy Efficiency and Renewable Energy, Building Technologies Office of the U.S. Department of Energy under Contract No. DE-AC02-05CH11231.